Temperature Dependence of Forward and Reverse Electron Transfer from A_1^-, the Reduced Secondary Electron Acceptor in Photosystem I†

Eberhard Schlodder,*,‡ Klaus Falkenberg,‡ Martin Gergeleit,‡ and Klaus Brettel*,§

Max-Volmer-Institut für Biophysikalische Chemie und Biochemie, Technische Universität Berlin, Strasse des 17. Juni 135, 10623 Berlin, Germany, and Section de Bioénergétique and CNRS, URA 2096, Département de Biologie Cellulaire et Moléculaire, CEA-Saclay, 91191 Gif-sur-Yvette Cedex, France

Received December 30, 1997; Revised Manuscript Received March 16, 1998

ABSTRACT: Electron-transfer reactions following the formation of $P700^+A_1^-$ have been studied in isolated Photosystem I complexes from *Synechococcus elongatus* between 300 and 5 K by flash absorption spectroscopy. (1) In the range from 300 to 200 K, A_1^- is reoxidized by electron transfer to the iron−sulfur cluster F_X. The rate slows down with decreasing temperature, corresponding to an activation energy of 220 ± 20 meV in this temperature range. Analyzing the temperature dependence of the rate in terms of nonadiabatic electron-transfer theory, one obtains a reorganization energy of about 1 eV and an edge-to-edge distance between A_1 and F_X of about 8 Å assuming the same distance dependence of the electron-transfer rate as in purple bacterial reaction centers. (2) At temperatures below 150 K, different fractions of PS I complexes attributed to frozen conformational substates can be distinguished. A detailed analysis at 77 K gave the following results: (a) In about 45%, flash-induced electron transfer is limited to the formation and decay of the secondary pair $P700^+A_1^-$. The charge recombination occurs with a $t_{1/2}$ of about 170 μs. (b) In about 20%, the state $P700^+F_X^-$ is formed and recombines with complex kinetics ($t_{1/2}$ = 5−100 ms). (c) In about 35%, irreversible formation of $P700^+F_A^-$ or $P700^+F_B^-$ is possible. (3) The transition from efficient forward electron transfer at higher temperatures to heterogeneous photochemistry at low temperatures has been investigated in different glass-forming solvents. The yield of forward electron transfer to the iron−sulfur clusters decreases in a narrow temperature interval. The temperature of the half-maximal effect varies between different solvents and appears to be correlated with their liquid to glass transition. It is proposed that reorganization processes in the surroundings of the reactants which are required for the stabilization of the charge-separated state become arrested near the glass transition. This freezing of protein motions and/or solvent reorganization may affect electron-transfer reactions through changes in the free-energy gap and the reorganization energy. (4) The rate of charge recombination between $P700^+$ and A_1^- increases slightly (about 1.5-fold) when the temperature is decreased from 300 to 5 K. This charge recombination characterized by a large driving force is much less influenced by the solvent properties than the forward electron-transfer steps from A_1^- to F_X and $F_{A/B}$.

Photosystem I (PS I)[1] of higher plants, algae, and cyanobacteria is a membrane-bound pigment−protein complex that mediates the light-driven electron transfer from reduced plastocyanin or cytochrome c_6 to ferredoxin or flavodoxin (for reviews, see refs 1 and 2). The PS I complex of *Synechococcus* is composed of 11 subunits. The two largest subunits (PsaA and PsaB of about 83 kDa each) form the heterodimeric core of PS I. They bind the antenna pigments (about 100 chlorophyll *a* and 20 β-carotene molecules) and the following redox cofactors involved in the electron-transfer process: the primary electron donor P700, a chlorophyll *a* (Chl *a*) dimer; the primary acceptor A_0, a Chl *a* monomer; the secondary acceptor A_1, a phylloquinone, also called vitamin K_1; and F_X, a [4Fe-4S] iron−sulfur cluster. The terminal electron acceptors F_A and F_B (two [4Fe-4S] iron−sulfur clusters) are both coordinated by subunit PsaC, one of the three extrinsic subunits located on the stromal side. Photosystem I can be isolated from cyanobacteria in a monomeric and trimeric form (*3*, *4*).

The structure of PS I has been determined to a resolution of 4 Å in a recent X-ray crystallographic study using crystals of trimeric PS I complexes of *Synechococcus elongatus* (*5*, *6*). The location of the three iron−sulfur clusters could be very well resolved. Six chlorophyll molecules have been assigned to the electron-transfer chain. These chlorophylls are arranged along two branches which are approximately related to each other by a 2-fold symmetry axis extending from F_X to a pair of chlorophylls located near the lumenal

†This work was supported by grants from the Deutsche Forschungsgemeinschaft, Sonderforschungsbereich 312, Teilprojekt A5 and by the Procope program.

* To whom correspondence should be addressed.

‡ Max-Volmer-Institut für Biophysikalische Chemie und Biochemie.

§ Section de Bioénergétique.

[1] Abbreviations: A_1, secondary electron acceptor in PS I (a phylloquinone); BV, benzyl viologen; CAPS, 3-(cyclohexylaminol-1-propanesulfonic acid); Chl *a*, chlorophyll *a*; *d*, optical path length for the measuring light; DPIP, 2,6-dichlorophenolindophenol; FeS, iron−sulfur cluster; F_X, F_A, and F_B, three [4Fe-4S] clusters in PS I; MES, 2-(*N*-morpholino)-ethanesulfonic acid; P700, primary electron donor in PS I (presumably a Chl *a* dimer); PMS, phenazine methosulfate; PS I, photosystem I; $t_{1/2}$, half-life.

S0006-2960(97)03182-6 CCC: $15.00
Published on Web 06/11/1998

side that presumably constitute the primary electron donor P700. In analogy to purple bacterial reaction centers, two additional Chls were assigned as monomeric accessory Chls. Next along each branch, chlorophyll monomers have been located at positions corresponding to those of the two bacteriopheophytins in bacterial reaction centers. One of them is assumed to be the primary electron acceptor A_0. The positions of the two phylloquinones present in PS I could not positively be identified in the electron density. Recently, information on the position and orientation of A_1 became available from magnetic resonance spectroscopy (*7*−*12*).

After absorption of light by an antenna pigment, the excitation energy is efficiently transferred to the primary electron donor. P700 in the lowest excited singlet state donates an electron to the primary acceptor A_0 within a few picoseconds. Subsequent charge stabilization is achieved by electron transfer from A_0^- to the secondary acceptor A_1 in about 30 ps. A half-life of 200 ns was found for the reoxidation of A_1^- in PS I complexes from *Synechococcus* (*13*), whereas in PS I from spinach, A_1^- decays biphasically with $t_{1/2} \cong 25$ and 150 ns and relative amplitudes depending on the preparation (*14*, *15*). Recent studies provided direct evidence that A_1^- is reoxidized by F_X (*16*−*18*). At low temperatures, the quantum yield of the electron transfer to the iron−sulfur clusters is diminished (10−20% at 10 K) (*19*). This indicates that the rate of forward electron transfer from A_1^- to the iron−sulfur clusters decreases as one lowers the temperature and that the charge recombination of the secondary radical pair, $P700^+A_1^-$, competes with the forward electron transfer. An intriguing aspect of the electron transfer of PS I is the reported heterogeneity at low temperature and in particular the observation that the forward electron transfer to the terminal iron−sulfur clusters is completely blocked in a fraction of PS I at 10 K (*19*).

In the present work, we study the temperature dependence of the electron reactions following the formation of the secondary pair $P700^+A_1^-$ throughout the full temperature range from 300 to 5 K in order to determine the parameters which control the electron transfer from A_1^- to the iron−sulfur clusters and to unravel the origin of the peculiar low-temperature effects on electron transfer in PS I. To investigate the influence of the solvent, these studies have been performed in different glass-forming media. Among others, our results indicate that reorganization processes in the medium surrounding PS I play an important role for the function of PS I under physiological conditions. Some of the results have been presented at the Xth International Congress of Photosynthesis (*20*).

MATERIALS AND METHODS

Samples. Trimeric PS I complexes with about 100 Chl/P700 were isolated from thermophilic cyanobacteria *S. elongatus* as described by Witt et al. (*21*). The material was stored in the dark at −30 °C.

For the measurements, the PS I complexes were thawed and diluted with buffer (either buffer A containing 20 mM Tricine (pH 8.2), 25 mM $MgSO_4$, and 0.02% *n*-dodecyl-*β*-D-maltoside or buffer B containing 20 mM MES/NaOH (pH 6.5), 10 mM $MgCl_2$, 20 mM $CaCl_2$, and 0.02% *n*-dodecyl-*β*-D-maltoside, which gave the same results within the margin of error). Glycerol was added as cryoprotectant to a final concentration of about 65% (v/v) glycerol in order to obtain a transparent glass at low temperatures. Additionally, 5 mM sodium ascorbate and 500 *μ*M DPIP were added. Under these conditions, P700 is fully reduced and all electron accceptors are oxidized prior to excitation. The samples were frozen in the dark using a variable temperature liquid nitrogen cryostat (DN 1704 from Oxford Instruments) or an optical cryostat cooled with liquid helium (He flow model from S.M.C. or CF1204 from Oxford Instruments). For some measurements at room temperature, glycerol was omitted or 100 *μ*M benzyl viologen was added as an electron acceptor. The experimental results were not affected by this difference.

The temperature dependence of the rate of charge recombination between $P700^+$ and A_1^- was measured under conditions of prereduced iron−sulfur clusters F_A and F_B. PS I complexes were suspended in a buffer containing 200 mM CAPS (pH 10), 25 mM $MgCl_2$, 0.02% *n*-dodecyl-*β*-D-maltoside, 65% (v/v) glycerol, and 20 mM sodium dithionite. Before freezing, the extent of prereduction of the terminal iron−sulfur clusters F_A and F_B was controlled by measuring the absorbance changes at 826 nm due to $P700^+$ at room temperature. Prereduction of F_A and F_B yields a decay kinetics with a $t_{1/2}$ of about 250 *μ*s that was assigned to the charge recombination between $P700^+$ and A_1^- (*22*).

Flash-induced absorbance changes as a function of temperature were additionally studied using other glass-forming solvents than glycerol (60% v/v ethyleneglycol and 50% v/v dimethyl sulfoxide) or different concentrations of the cryoprotectant glycerol (between 50% and 85% v/v).

Spectroscopic Methods. The Chl/P700 ratio for the PS I complexes was calculated from the flash-induced absorption change at 703 nm due to the photooxidation of P700, using a differential molar extinction coefficient of 64 000 M^{-1} cm^{-1}.

Measurements of absorbance changes around 385 nm in the nanosecond time range were performed with the setup described in ref 23. The sample was excited by laser flashes of 3 ns pulse duration (fwhm) at 532 nm. A total sweep of up to 5 *μ*s was accessible using a Xe flashlamp as measuring light source. For measurements in the time range up to 4 ms, the measuring light from a 250 W tungsten halogen lamp (Osram) or a DC xenon arc lamp (XBO 150W/1) was pulsed by means of a photoshutter (open for ≤ 10 ms). The detector (S1723-02 Si photodiode from Hamamatsu), loaded with 5 or 10 kΩ, was coupled to an amplifier (TEK AM502 from Tektronix). The overall electrical bandwidth was DC-150 kHz with a load resistor of 5 kΩ.

The $P700^+A_1^-/P700A_1$ absorbance difference spectrum at 77 K was measured with a flash photometer that is characterized by a time resolution ($t_{10/90}$) of about 20 *μ*s. The measuring light of a 250 W tungsten halogen lamp (Osram) passed through a monochromator with 7 nm bandwidth placed between light source and sample and a combination of interference filters and colored glasses in front of the photomultiplier (EMI 9558BQ). The signals were digitized and averaged by a transient recorder (Biomation 4500 from Gould). The samples were excited by a saturating Xe flash of about 10 *μ*s duration filtered by colored glasses.

Absorbance changes at 826 nm in the nanosecond time range were measured as previously described (*24*). In the microsecond and millisecond ranges, a 250 W tungsten halogen lamp (Osram) was used as measuring light source.

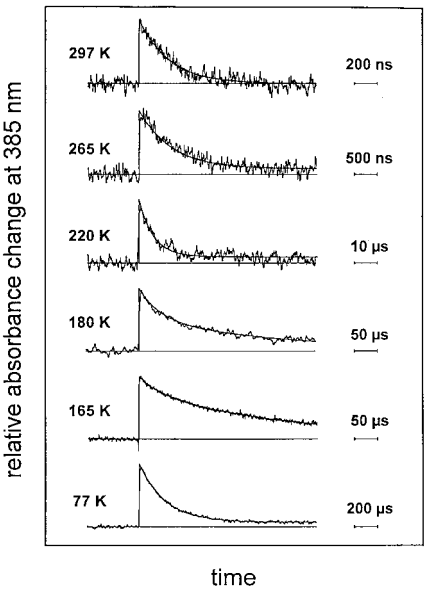

FIGURE 1: Flash-induced absorbance changes at 385 nm attributed to the formation and decay of A_1^- in PS I complexes from *Synechococcus elongatus* at different temperatures (note the different time scales). The signals (between 64 and 512 averages at repetition rates between 0.03 and 1 Hz) are normalized to their initial amplitudes. Conditions: 100 μM chlorophyll, $d = 0.12$ cm. A plexiglass cuvette was positioned at 45° to the mutually perpendicular exciting and measuring beams. At 297 K, the initial amplitude of the flash-induced absorbance change was 9.5×10^{-4} corresponding to a differential molar extinction coefficient of about 8000 M^{-1} cm^{-1}. At lower temperatures, the amplitudes depend on the excitation rate, since the states $P700^+F_A^-$ and $P700^+F_B^-$ accumulate to some extent due to their long lifetimes. The amplitude at 180 K, for example, was 6.1×10^{-4} at a repetition rate of 0.5 Hz.

The measuring light was monitored by a Si photodiode (SGD 444 from EG&G or OSD-100-5T from Centronic) with a load resistor of 1 kΩ coupled to the amplifier TEK AM 502 from Tektronix.

The time course of the absorption changes was fitted to a (multi)exponential decay using an algorithm that minimizes the sum of the unweighted least squares.

RESULTS

Flash-induced absorbance changes at 385 nm were measured at different temperatures between 300 and 77 K in order to analyze the temperature dependence of the reoxidation kinetics of A_1^-. At this wavelength, the absorbance changes are predominantly due to the formation and the decay of A_1^- (*13*). Figure 1 shows the time course of the absorbance changes at selected temperatures. At room temperature we observed a monoexponential decay with a half-life of 180 ns (upper trace in Figure 1; the solid line represents the fit), in good agreement with our previous measurements (*13, 16*). The rate of A_1^- reoxidation slowed with decreasing temperature. The lower the temperature, the longer was the time scale that had to be used in order to follow the decay of the flash-induced absorbance increase (note the different time scales in Figure 1). At 220 K, the decay could be fitted using one exponential with $t_{1/2} = 4.5$ μs. In the range from 200 to 150 K, two exponentials were required for a satisfactory fit. This is evident from the signal at 180 K which can be described by the following half-lives and relative amplitudes: 27 μs (46%) and 211 μs (54%). Decreasing the temperature from 200 to 150 K, the relative amplitude of the slower phase increased at the expense of the faster phase. Below 150 K, the fast phase could no longer be detected and the signals were dominated by the phase with a nearly temperature-independent $t_{1/2}$ of about 200 μs. The decay at 77 K could be fitted by a single exponential with $t_{1/2} = 170$ μs (see lowest trace in Figure 1).

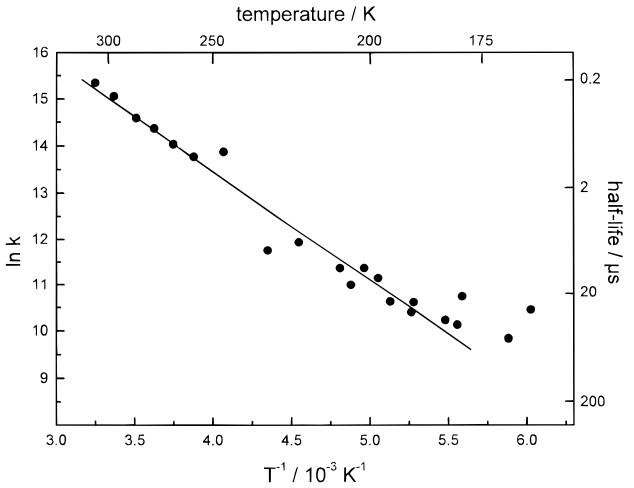

FIGURE 2: Arrhenius plot of the rate constant attributed to the forward electron transfer from A_1^- to F_X derived from measurements of flash-induced absorbance changes at 385 nm. For details see text.

Figure 2 shows an Arrhenius plot of the temperature dependence of the rate of A_1^- reoxidation in the range between 310 and 150 K; below 200 K only the rate constant of the fast phase of the biexponential fit was included. From comparisons with the kinetics of $P700^+$ (see next paragraph and Figure 3), it can be concluded that the rate constants plotted in Figure 2 are due to electron transfer from A_1^- to the iron−sulfur clusters and are not due to charge recombination between A_1^- and $P700^+$ (see below). In the range between 310 and 190 K, the data are reasonably described by a straight line yielding an activation energy of 220 ± 20 meV.

To clarify whether the reoxidation of A_1^- occurs by forward electron transfer to the iron−sulfur clusters or by charge recombination with $P700^+$, we measured absorbance changes at 826 nm reflecting formation and decay of $P700^+$ as a function of temperature. To allow comparison between the measurements at 826 and 385 nm, the absorbance changes at 826 nm were measured under repetitive excitation after preillumination. Between room temperature (not shown) and 200 K (Figure 3, upper trace), the kinetics of $P700^+$ reduction turned out to be much slower than the reoxidation of A_1^- (see Figure 1) excluding charge recombination between $P700^+$ and A_1^-. Decreasing the temperature below 200 K, an increasing fraction of $P700^+$ was reduced with kinetics comparable to the slower one of the two reoxidation phases of A_1^-, indicating that forward electron transfer became partially replaced by charge recombination of A_1^- with $P700^+$. At 77 K (Figure 3, 77 K trace), 83% of $P700^+$ decayed with the same half-life as observed for the reoxidation of A_1^- (Figure 1, lower trace). At 5 K, this phase accounts for about 87% of the $P700^+$

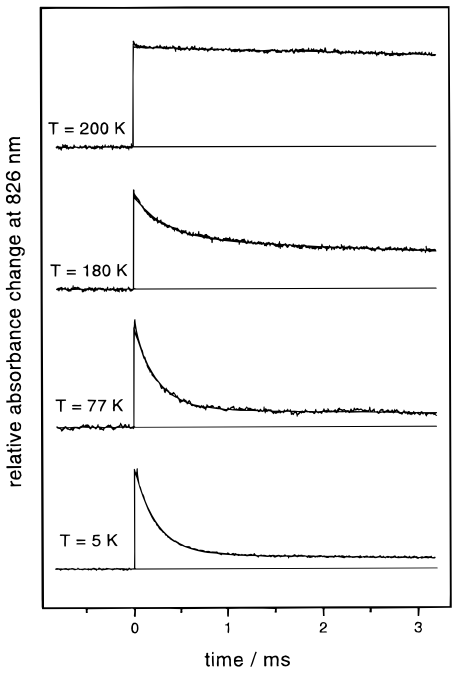

FIGURE 3: Flash-induced absorbance changes at 826 nm attributed to the formation and decay of $P700^+$ at selected temperatures measured under repetitive excitation. The repetition rate was 0.5 Hz. The signals are normalized to their initial amplitudes. Conditions: 30 μM chlorophyll, $d = 1$ cm. The absorbance change induced by the first flash was 2.4×10^{-3}. Under repetitive excitation, the absorbance change depends on the excitation rate and the lifetimes of the states $P700^+F_A^-$ and $P700^+F_B^-$. The amplitude at 77 K, for example, was 1.5×10^{-3} at a repetition rate of 1 Hz.

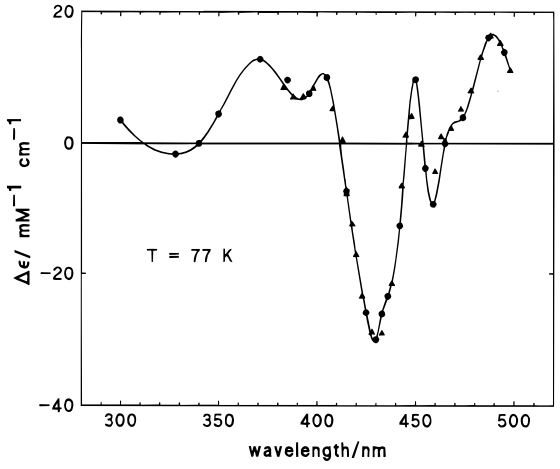

FIGURE 4: Spectrum of flash-induced absorption changes decaying with a half-life of 170 μs in PS I complexes from *Synechococcus* at 77 K. Conditions: 10 μM chlorophyll, $d = 1$ cm.

decay. Therefore, this phase is attributed to charge recombination of $P700^+A_1^-$ being the dominant reversible process at cryogenic temperatures. This conclusion is supported by the spectrum of the 170 μs decay phase shown in Figure 4 that was measured at 77 K between 300 and 500 nm. The spectrum resembles closely the $P700^+A_1^-/P700A_1$ difference spectrum measured at 10 K in spinach PS I under conditions of prereduced F_A and F_B (*25*). The absorbance increase in the range from 350 to 400 nm is mainly due to the reduction of A_1, whereas the bleaching around 430 nm mainly reflects the oxidation of P700 (*26*).

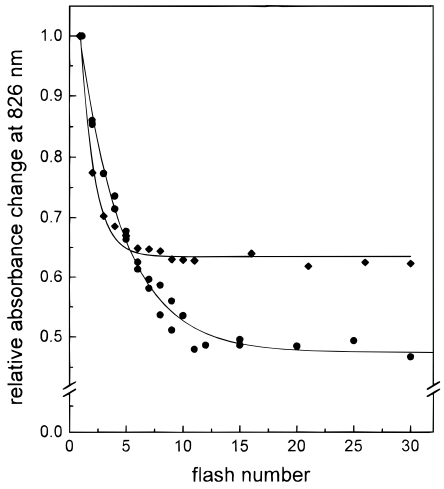

FIGURE 5: Relative initial amplitudes of the flash-induced absorbance change at 826 nm as function of the flash number at 5 K (●) and 77 K (◆). The samples were dark-adapted before freezing in the presence of 5 mM ascorbate. Conditions: 30 μM chlorophyll, $d = 1$ cm. The absorbance change induced by the first flash was 2.4×10^{-3}. The solid lines represent the best fits using the function $\Delta A_n = (\Delta A_1 - \Delta A_r)\Phi^{n-1} + \Delta A_r$ as described in the text. The following values for the parameters were obtained: at 77 K, $\Delta A_r = 0.63$ and $\Phi = 0.55$; at 5 K, $\Delta A_r = 0.47$ and $\Phi = 0.22$.

The absorbance changes which did not decay on the 3 ms time scale shown in Figure 3 represent the longer-lived charge-separated states $P700^+F_X^-$, $P700^+F_A^-$, and $P700^+F_B^-$. The relative amplitudes of these longer-lived absorbance changes decreased from virtually 100% above 200 K to about 15% below 150 K. At 77 K, the small longer-lived absorbance change (see Figure 3, lower trace) decayed multiphasically with half-lives between 5 and 100 ms (not shown). The difference spectrum of these long-lived absorbance changes was measured in the range between 300 and 500 nm. It was similar to those attributed to the decay of $P700^+F_X^-$ at 77 K in PS I core complexes devoid of F_A and F_B (*16*). It is known from the literature that $P700^+F_A^-$ and $P700^+F_B^-$ can be formed at low temperature in some fraction of the PS I complexes (*19*, *27*) and presumably give rise to similar difference spectra. However, these states are stable for hours below 100 K and cannot be observed in the low-temperature experiments described above which were performed under repetitive excitation after preillumination. The fraction of the PS I complexes, which is capable of electron transfer to F_A or F_B, is trapped in the stable states $P700^+F_A^-$ and $P700^+F_B^-$ due to the preillumination and cannot perform photochemistry in subsequent flash experiments (see next section). Therefore, we attribute the multiphasic decay with $t_{1/2} = 5-100$ ms exclusively to the charge recombination of $P700^+F_X^-$. The multiphasic kinetics of the recombination may indicate the presence of different conformational substates of PS I at low temperature.

To determine the size of the fraction which is capable of electron transfer to F_A and F_B in the PS I preparation from *Synechococcus* used in this study, samples frozen in the dark to 77, 50, 20 or 5 K were exposed to a series of saturating flashes. The initial amplitudes of the absorbance change at 826 nm induced by a single flash out of the series are plotted in Figure 5 as a function of the flash number for 77 K (diamonds) and 5 K (circles). The observed decrease of the initial amplitude is caused by the irreversible formation of

either state $P700^+F_A^-$ or state $P700^+F_B^-$. The fraction of the PS I complexes trapped in these states after 30 flashes was 37% at 77 K in the experiment shown in Figure 5. In the average of several experiments using different samples, a value of 35% ± 10% was observed. Further flashes or continuous illumination did not significantly increase this fraction, indicating that, in about 65% of the PS I complexes, electron transfer to the terminal iron−sulfur clusters is blocked at 77 K. Similar results were obtained with thylakoid membranes from *Synechococcus* (not shown). Decreasing the temperature slightly increased the fraction of PS I complexes which could be trapped in long-lived states (up to about 50% at 5 K compared to 35% at 77 K (see Figure 5)). It is of note that the energy of the excitation flashes used in these experiments was saturating; that is, all PS I centers were excited by each flash. Nevertheless, several successive flashes were required to obtain the maximal decrease of the initial amplitude, that is, to form $P700^+F_A^-$ or $P700^+F_B^-$ in the entire fraction of PS I complexes capable of electron transfer to F_A or F_B. This indicates that, in this fraction, electron transfer to the iron−sulfur clusters is inefficient at low temperature (see discussion). The solid lines in Figure 5 are the best fits using the following fit function:

$$\Delta A_n = (\Delta A_1 - \Delta A_r)\Phi^{n-1} + \Delta A_r$$

with ΔA_n = absorbance change induced by the nth flash, ΔA_r = remaining absorbance change after several (>50) flashes, and Φ = quantum yield for the formation of long-lived states in that fraction of PS I complexes, which is capable of transferring an electron to F_A and F_B. The fit parameters are given in the figure legend and will be discussed below.

The reversible absorbance changes observed at $T < 100$ K after preillumination exhibited kinetic phases with $t_{1/2} \cong 170$ μs (≈85%) and $t_{1/2} > 5$ ms (≈15%) (see Figure 3, lower traces) attributed to the charge recombination of the pairs $P700^+A_1^-$ and $P700^+F_X^-$, respectively. The observation of $P700^+A_1^-$ recombination might result either from the competition between forward electron transfer from A_1^- to F_X and charge recombination of $P700^+A_1^-$ or from a heterogeneity with respect to the electron transfer from A_1^- to F_X (in addition to the heterogeneity described above), that is, from the presence of a fraction of PS I complexes in which the electron transfer from A_1^- to F_X is blocked. To address this issue, we studied the influence of background illumination on the flash-induced absorbance changes. Figure 6 shows the results obtained at 77 K. Increasing the intensity of the background illumination, the initial amplitude of the flash-induced absorbance changes decreased. This was expected because the charge-separated states (mainly the longest-lived state $P700^+F_X^-$) are populated already to some extent by the background illumination so that the flash cannot induce a charge separation. However, deviating from the expected behavior for a homogeneous photochemistry (see discussion), the initial amplitude of the flash-induced absorbance changes decreased biphasically as a function of the intensity of the background illumination (see Figure 6, inset). The relative amplitudes of the two components were about 30% and 70%, and the ratio of the half-saturating intensities was about 1:200. The slower phase of the $P700^+$ decay

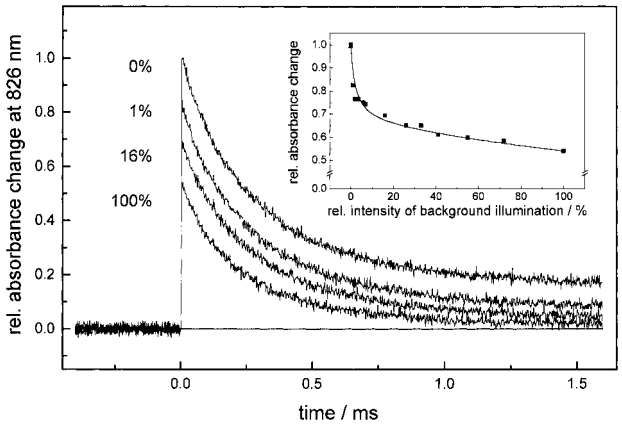

FIGURE 6: Influence of background illumination on the flash-induced absorbance changes at 826 nm of PS I complexes from *Synechococcus* at 77 K. The inset shows the initial amplitude of the flash-induced absorbance changes as a function of the intensity of the background illumination. The solid line has been calculated using the function

$$\Delta A = \Delta A_B\left(\frac{1}{1 + I/I_{1/2}^B}\right) + \Delta A_C\left(\frac{1}{I + I/I_{1/2}^C}\right)$$

in order to account for the biphasic decrease of ΔA attributed to the different PS I fractions B and C. $I_{1/2}$ corresponds to k^*/σ in eq 4. See text for details. The parameters are $\Delta A_B = 0.34$, $I_{1/2}^B = 2\%$, $\Delta A_C = 0.66$, and $I_{1/2}^C = 420\%$.

disappeared first with increasing intensity (see Figure 6, upper three traces). Much higher intensities were required to halve the amplitude of the faster phase (see Figure 6, lowest trace). These results give evidence for a strong heterogeneity with respect to the electron transfer from A_1^- to F_X. Only in a fraction of the PS I complexes, electron transfer from A_1^- and F_X is efficient. In this fraction, a high steady-state population of $P700^+F_X^-$ is obtained already at relatively low intensities of background illumination, because the lifetime of the state $P700^+F_X^-$ is rather long ($t_{1/2} = 5-100$ ms). This explains the high sensitivity of the slower phase of the $P700^+$ decay to background illumination. In a larger fraction of the PS I complexes, electron transfer from A_1^- and F_X is inefficient and the state $P700^+A_1^-$ decays essentially by charge recombination. Due to its much shorter lifetime ($t_{1/2} \cong 170$ μs), much higher intensities of background illumination are required to obtain a high steady-state population of $P700^+A_1^-$.

On the basis of the described results, we can distinguish at least three fractions of the PS I complexes at 77 K. A rough estimation yielded that, in about 45% of the PS I complexes, only the state $P700^+A_1^-$ can be formed; in about 20% the formation of $P700^+F_X^-$ is possible without further forward electron transfer, and in about 35% the electron transfer can proceed up to F_A or F_B giving rise to the trapped states $P700^+F_A^-$ and $P700^+F_B^-$ as described above. These percentages were estimated using ΔA_r from Figure 5 and the amplitude ratio of the two components in the inset of Figure 6.

The effect of background illumination was also studied at higher temperatures (not shown). The results indicate that the photochemistry becomes heterogeneous below approximately 200 K.

The experiments described so far were performed in the presence of 65% (v/v) glycerol in order to obtain a transpar-

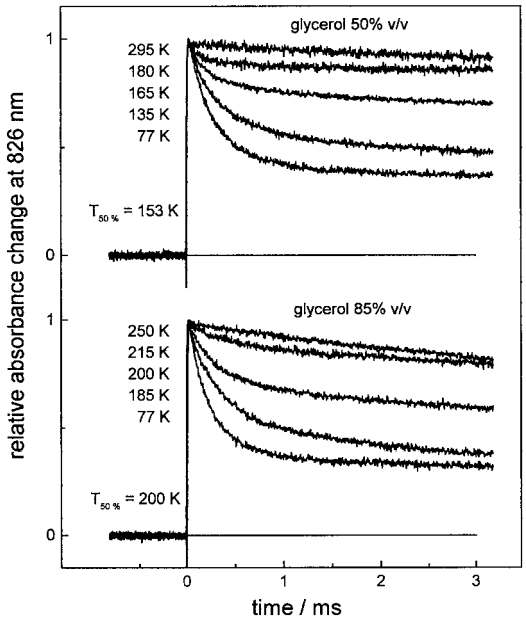

FIGURE 7: Absorbance changes at 826 nm induced by the first flash given to PS I complexes from *Synechococcus* frozen in the dark. The experiments were performed in the presence of 50% (upper traces) and 85% glycerol (lower traces). The traces are for the temperatures (from top to bottom) 295, 180, 165, 135, and 77 K (50% glycerol) and 250, 215, 200, 185, and 77 K (85% glycerol).

ent glass at low temperature. According to Rasmussen and MacKenzie (*28*), the liquid to glass transition of this medium occurs at approximately 170 K, that is, in the temperature range where we observed the breakdown of efficient forward electron transfer to the iron−sulfur clusters and the appearance of heterogeneity. To analyze the influence of the solvent, we studied the temperature dependence of the efficiency of forward electron transfer beyond A_1 in media with different glass-transition temperatures. As examples, the top and bottom panels in Figure 7 show absorbance changes at 826 nm induced by the first flash given to PS I complexes frozen in the dark in the presence of 50% and 85% glycerol, respectively. Similar to results in the presence of 65% glycerol shown in Figure 3 for repetitive excitation, the amplitude of the slow decay of $P700^+$ ($t_{1/2} > 1$ ms) which is a measure of the yield of forward electron transfer to the iron−sulfur clusters decreased in a narrow temperature interval. The temperature dependence of this yield is shown in Figure 8 for both media. The temperature of the half-maximal effect ($T_{50\%}$) was about 150 K at 50% glycerol and about 200 K at 85% glycerol. Table 1 summarizes the results for different glass-forming media. For comparison, published glass-transition temperatures, T_g, for pure solvent−water mixtures are also given in Table 1. These T_g values may not apply exactly for our experiments, since the presence of other components (buffer, salts, PS I complexes, etc.) and different cooling rates might influence the glass-transition temperature. Nevertheless, the variation of the $T_{50\%}$ values between the different media turned out to be roughly parallel to the variation of the T_g values for the pure solvent−water mixtures.

We also checked whether the charge recombination between $P700^+$ and A_1^- which is in competition with forward electron transfer to F_X is affected by the glass transition of the medium as well. To follow the $P700^+A_1^-$ charge recombination rate over the whole temperature range from

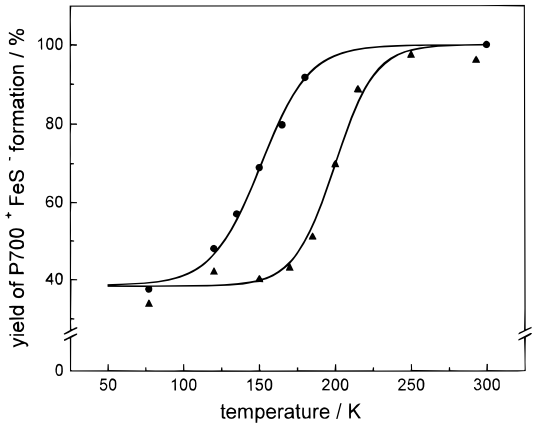

FIGURE 8: Temperature dependence of the yield of forward electron transfer to the iron−sulfur clusters measured in the presence of 50% (●) and 85% glycerol (▲). The temperature of the half-maximal effect ($T_{50\%}$) was 153 K at 50% glycerol and 198 K at 85% glycerol.

Table 1: Characteristic Temperatures ($T_{50\%}$) at which the Yield Y of Forward Electron Transfer beyond A_1^- Decreases in Different Glass-Forming Media[a]

solvent	$T_{50\%}$/K	T_g/K
dimethylsulfoxide 50% v/v	141	143[b]
ethyleneglycol 60% v/v	154	149[c]
glycerol 50% v/v	151	158[d]
glycerol 65% v/v	168	167[d]
glycerol 85% v/v	199	181[d]

[a] The decrease of the yield upon lowering the temperature has been fitted with the following function (see solid lines in Figure 8 as an example):

$$Y = \min + \frac{\max - \min}{1 + \exp(-\xi(T - T_{50\%}))}$$

The Table summarizes the temperatures of the half-maximal effect ($T_{50\%}$) obtained by these fits. The glass transition temperatures (T_g) for the pure solvent−water mixtures taken from the literature are indicated for comparison. [b] Data from Rasmussen and MacKenzie (*28*). [c] Data from Iben et al. (*30*). [d] Data from Rasmussen and MacKenzie (*29*).

77 to 300 K, F_A and F_B were prereduced by dithionite at pH 10 in these experiments (*22*). Measurements of the charge recombination at low temperature without prereduction of F_A and F_B (Figure 3, lower traces) yield the same rate within the limits of error. As shown in Figure 9, the observed rate depends only weakly on the temperature and the glycerol concentration of the medium. Lowering the temperature from 300 to 5 K (see Figure 9 and Figure 3), the rate increased slightly, in accordance with previous results (*19*, *31*). A deviation from this trend is visible between 200 and 140 K (Figure 8). It cannot be decided from the data whether there is a correlation between this feature and the glass-transition temperatures of the three media used.

DISCUSSION

To assign the observed kinetics of the A_1^- oxidation to molecular rate constants, we consider the general kinetic Scheme 1 for the reactions following the formation of the secondary radical pair $P700^+A_1^-$.

Electron Transfer above 200 K. Above 200 K, A_1^- was found to be reoxidized virtually exclusively by electron transfer to the iron−sulfur clusters, as evidenced by the absence of $P700^+$ decay on the time scale of A_1^- reoxidation

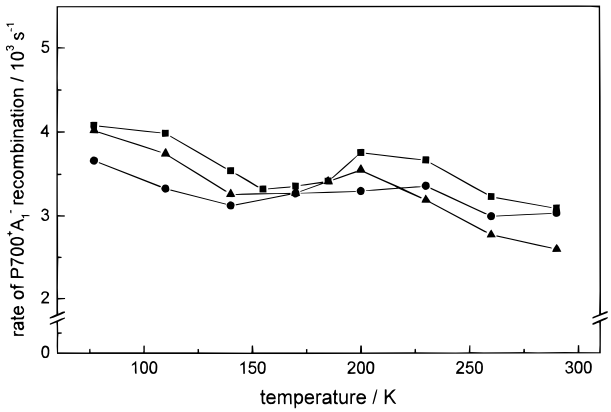

FIGURE 9: Temperature dependence of the rate of $P700^+A_1^-$ charge recombination in PS I complexes from *Synechococcus* measured under conditions of prereduced terminal iron−sulfur clusters F_A and F_B (pH 10, 20 mM sodium dithionite). Measurements were performed in the presence of 50% (●), 65% (■), and 85% glycerol (▲).

Scheme 1

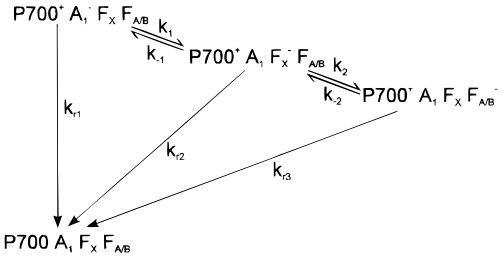

(compare Figures 1 and 3). Hence, $P700^+A_1^-$ recombination does not contribute to the decay of A_1^- (i.e., rate constant $k_{r1} \ll k_1$ at $T > 200$ K).

The nearly monoexponential decay of A_1^- suggests that the forward electron-transfer rate k_1 is considerably larger than the reverse rate k_{-1} (i.e., $k_1 \gg k_{-1}$ and $\Delta G°$ ($P700^+A_1^-F_X \rightarrow P700^+A_1F_X^-$) $= -RT \ln(k_1/k_{-1}) < 0$). A different possibility to explain the monoexponential oxidation kinetics of A_1^- would be to assume that $k_2 \gg k_{-1}$, k_{-2}. Under this assumption k_1 needs not to be larger than k_{-1}, that is, $\Delta G°$ might even be positive. For a detailed discussion of the energetics of the electron-transfer reactions in PS I see ref 2. In both cases ($k_1 \gg k_{-1}$ and $k_2 \gg k_{-1}$, k_{-2}) the observed rate of A_1^- oxidation can be identified with k_1 as a good approximation.

In the following we discuss the observed temperature dependence of the A_1^- oxidation rate k_1 in terms of nonadiabatic electron-transfer theory. According to the classical Marcus theory, the rate of a nonadiabatic electron-transfer reaction can be expressed as (*32*)

$$k = \frac{2\pi|V|^2}{\hbar\sqrt{4\pi\lambda k_B T}} \exp\left[\frac{-(\Delta G° + \lambda)^2}{4\lambda k_B T}\right] \qquad (1)$$

where V is the electronic coupling of the reactants and the products electronic states. To a first approximation, V decreases exponentially with the edge-to-edge distance R between the reactants. λ is the reorganization energy and $\Delta G°$ is the standard Gibbs free energy of reaction. Because of the mutual dependency of the parameters $\Delta G°$ and λ, the data shown in Figure 2 were fitted using fixed and temperature-independent $\Delta G°$ values. Although the $\Delta G°$ value of the reaction is not precisely known, different estimates suggest a value in the range between −0.1 and +0.06 eV (for a discussion of published data see ref 2). To accommodate for the observed strong temperature dependence of the rate of A_1^- oxidation kinetics, $-\Delta G°$ must be small compared to λ. In this case, the uncertainty in $\Delta G°$ has relatively small effects on the calculated values of V and λ. The fit yielded reorganization energies between 0.8 and 1.1 eV and an electronic coupling between 1.0 and 1.12 meV (8 and 9 cm^{-1}) varying $\Delta G°$ from +0.06 to −0.1 eV. These parameters correspond to an optimal rate k_{op} (calculated for $-\Delta G° = \lambda$ at $T = 295$ K) of 2×10^{10} s^{-1}.

The use of the classical expression (eq 1) is justified when the energies of vibrational modes coupled to the electron transfer are small compared to the thermal energy k_BT. Moser et al. (*33*) have shown that the $\Delta G°$ and temperature dependence of several electron-transfer reactions in bacterial reaction centers can be described assuming a common characteristic frequency ($\hbar\omega \approx 70$ meV $\approx 3k_BT$ at room temperature) which was attributed to protein high-frequency vibrational modes. Therefore, we tried to analyze our data in terms of a quantum mechanical treatment of nonadiabatic electron transfer. To simplify calculations, we used an expression with a single vibration coupled to the electron transfer (*32*, *34*).

$$k = \frac{2\pi|V|^2}{\hbar^2\omega} \exp[-S(2n+1)]\left(\frac{n+1}{n}\right)^{p/2} I_p(2S\sqrt{n(n+1)}) \qquad (2)$$

where

$$S = \frac{\lambda}{\hbar\omega},\ p = \frac{-\Delta G°}{\hbar\omega},\ n = \left(\exp\left[\frac{\hbar\omega}{k_B T}\right] - 1\right)^{-1}, \quad \text{and}$$

$$I_p(Z) = \sum_{k=0}^{\infty} \frac{(Z/2)^{p+2k}}{k!\Gamma(p+k+1)}$$

is the modified Bessel function of order p (extended to noninteger values of p).

Attempts to fit our data for $T > 200$ K with a fixed value of $\hbar\omega = 70$ meV and reasonable $\Delta G°$ values (see above) yielded reorganization energies between 1.6 and 2.0 eV and an electronic coupling corresponding to an optimal rate k_{op} (calculated for $-\Delta G° = \lambda$ at $T = 295$ K) of about 8×10^{12} s^{-1}. Such a high optimal rate could only be expected if A_1 and F_X were almost at van der Waals contact (*33*). This is, however, inconsistent with the recently estimated center-to-center distance of 14 ± 2 Å (*6*, *10*). Furthermore, the reorganization energies obtained by these fits are unreasonably high (see below). To fit the data with more realistic parameters, one has to assume a lower characteristic frequency of the vibrations coupled to the electron transfer from A_1^- to F_X. For example, for $\hbar\omega = 25$ meV the fit yielded λ values between 0.8 and 1.1 eV and V values between 1.0 and 1.4 meV ($\Delta G°$ was again varied between +0.06 and −0.1 eV). The optimal rates were similar to that obtained by the analysis of the temperature dependence of the rate with the classical Marcus equation, that is, $k_{op} \cong 2 \times 10^{10}$ s^{-1}.

We conclude from these considerations that electron transfer from A_1^- to F_X is coupled to lower-frequency vibrational modes than the electron tranfer in bacterial reaction centers analyzed by Moser et al. (*33*) and that the classical Marcus equation provides a reasonable description of electron transfer from A_1^- to F_X above 200 K. From the optimal electron-transfer rate (k_{op}) derived above, one may estimate the edge-to-edge distance between A_1 and F_X using the empirical relation $\log k_{op} = 15 - 0.6R$ (with k_{op} in s^{-1} and R in Å) which was shown to be a good approximation for some twenty intraprotein electron-transfer reactions over distances between 5 and 23 Å (*35*). Inserting $k_{op} = 2 \times 10^{10}$ s^{-1} one obtains $R = 7.8$ Å.

This edge-to-edge distance should be compared with the recently reported distance of 14 ± 2 Å between the midpoint of the carbonyl oxygens of the phylloquinone A_1 and the center of F_X (*6*, *10*). The edge-to-edge distance depends sensitively on the orientation of the phylloquinone double ring relative to F_X. Magnetic resonance data led to the conclusion that the vector connecting P700 and A_1 is roughly parallel to the C═O bonds (*12*, *36*) and that the phylloquinone double ring is approximately coplanar with the triangle P700−A_1−F_X (*37*). Two possibilities remain. (a) The benzyl ring of the phylloquinone A_1 is oriented toward F_X; among the atoms involved in the conjugated π-electron system of phylloquinone, the carbon atom C6 would be closest to F_X for this case. (b) The phylloquinone is rotated in-plane by 180° around the midpoint of the two carbonyl oxygens, so that C2 would be closest to F_X. In this orientation the edge-to-edge distance would be about 2.3 Å larger than for case (a). Taking into account the dimensions of A_1 and F_X (*15*, *38*, *39*), our estimate of the edge-to-edge distance between A_1 and F_X fits well with a center-to-center distance of 14 Å if orientation (a) is realized. However, the alternative orientation of A_1 cannot be completely excluded because of the rather large error margins and uncertainties in the above estimations.

The outer reorganization energy, λ_o, for electron transfer from from A_1^- to F_X can be calculated using the following expression (*32*, *39*)

$$\lambda_o = e^2\left(\frac{1}{\epsilon_{op}} - \frac{1}{\epsilon_s}\right)\left(\frac{1}{2r_{eff1}} + \frac{1}{2r_{eff2}} - \frac{1}{r_{cc}}\right) \qquad (3)$$

where e is the elementary charge, ϵ_{op} and ϵ_s are the optical and static dielectric constants of the medium, respectively, r_{eff1} and r_{eff2} are the effective radii of the reactants (see ref 15 for a discussion), and r_{cc} is the distance between their centers. The medium surrounding the reactants is assumed to be homogeneous. Using a center-to-center distance of 14 Å, eq 3 provides a lower and upper limit for the outer reorganization energy of 0.45 and 1.6 eV, assuming dielectric constants characteristic for hydrophobic proteins with dielectric properties as suggested by Krishtalik (*39*) and for water, respectively. The inner reorganization energy is unlikely to exceed 0.1 eV for electron transfer between molecules as large as phylloquinone and [4Fe-4S] clusters (*39*). Our value of about 1 eV for the total reorganization energy derived by the analysis of the electron transfer from A_1^- to F_X indicates that the polarizability of the surroundings of the reactants must be significantly larger than that of a hydrophobic protein.

The basic assumption for the analysis of the A_1^- reoxidation rate in terms of electron-transfer theory was that the observed rate can be identified with the molecular rate constant k_1. It should be noted that this is not necessarily the case. One possibility that has not been discussed above is a rapid preequilibrium between $A_1^-F_X$ and $A_1F_X^-$ that decays by slower electron transfer to $F_{A/B}$, that is, $k_2 \ll k_1 + k_{-1}$ and $k_2 \gg k_{-2}$. In this case, A_1^- decays nearly monoexponentially when $k_1 \ll k_{-1}$ and the observed rate is given by $k_2K/(1 + K)$ with $K = k_1/k_{-1}$. The temperature dependence of the observed rate would then reflect the temperature dependence of k_2 and of K. The formation of the state $P700^+A_1F_X^-$ with high yield in PS I core complexes depleted of F_A and F_B shows that k_1 must be larger than k_{-1} contrary to the possibility mentioned above. However, it has been suggested (*2*) that removal of stromal extrinsic subunits during depletion of F_A and F_B might increase the redox potential of F_X and hence increase K, so that the case $k_1 < k_{-1}$ cannot be safely excluded for intact PS I.

Electron Transfer below 200 K. Lowering the temperature from 200 to 150 K, we observed that forward electron transfer from A_1^- to the iron−sulfur clusters was increasingly replaced by charge recombination with $P700^+$. Below 150 K, about 60% of $P700^+A_1^-$ induced by the first flash decayed by charge recombination with $t_{1/2} = 150-200$ μs (see Figures 7 and 8). At a first glance, this observation might be explained by a further decrease of rate constant k_1 (see Scheme 1) between 200 and 150 K so that the charge recombination (k_{r1}) can compete with forward electron transfer from A_1^- to F_X. Since k_{r1} is hardly dependent on temperature (see Figure 9), k_1 would have to be constant at a value of about 2×10^3 s^{-1} below 150 K in order to explain the temperature-independent yield ($=k_{r1}/(k_1 + k_{r1}) \cong 0.6$) of $P700^+A_1^-$ recombination with $t_{1/2} = \ln 2/(k_1 + k_{r1}) \cong 200$ μs at $T < 150$ K.

Unfortunately, this simple explanation alone is not sufficient to account for the results obtained by successive flashes (Figure 5) or for the effects of background illumination (Figure 6). The observation that only a fraction (e.g., about 35% at 77 K in the PS I preparation from *S. elongatus* used in this study) could be trapped in the quasi-irreversible state $P700^+F_{A/B}^-$ by a large number of flashes (see Figure 5) provides strong evidence for a functional heterogeneity of PS I at low temperatures: only in this fraction of the PS I complexes (called fraction A in the following) forward electron transfer from A_1^- via F_X to F_A and F_B can compete with the charge recombination reactions (k_{r1} and k_{r2} in Scheme 1). A single saturating flash given to a sample frozen in the dark achieved approximately 50% of the maximally possible formation of $P700^+F_{A/B}^-$ at 77 K (see Figure 5). It is obvious from Scheme 1 that this is possible only if $k_1 \geq k_{r1} \cong 2 \times 10^3$ s^{-1} in fraction A. The size of this fraction increases slightly (to about 50% (see Figure 5)) if the temperature is lowered to 5 K. This may indicate that at 77 K the state $P700^+F_{A/B}^-$ formed by a series of flashes or continuous illumination decays to some extent by slow recombination. In a study on PS I particles from spinach, Sétif et al. (*19*) observed that about 65% of the PS I centers were progressively trapped in the state $P700^+F_{A/B}^-$ by successive laser flashes at 10 K.

The effects of background illumination on samples where fraction A had already been trapped in the state $P700^+F_{AB}^-$

(Figure 6) provide evidence for yet another functional heterogeneity.

Assuming a homogeneous photochemistry in the PS I complexes which are unable to reduce F_A or F_B and undergo reversible charge separation at low temperature, the amplitude of flash-induced $P700^+$ should decrease with increasing background light intensity I according to the following equation:

$$\Delta A = \Delta A_{max}\left(\frac{1}{1 + \sigma \cdot I/k^*}\right) \quad (4)$$

$\sigma \cdot I$ is the excitation rate where σ is the effective absorption cross section. k^* is given by

$$k^* = \frac{k_{-1} + k_{r2}}{k_1 + k_{-1} + k_{r2}} k_{r1} + \frac{k_1}{k_1 + k_{-1} + k_{r2}} k_{r2}$$

(see Scheme 1 for the meaning of the rate constants). These relations are easily derived by calculating the steady-state concentrations in a modified Scheme 1 with $k_2 = 0$ and formation of $P700^+A_1^-$ from P700 A_1 with rate constant $\sigma \cdot I$. Equation 4 predicts a simple hyperbolic decrease of ΔA with increasing background light intensity I. ΔA is halved when the excitation rate equals k^*, which may be considered as an effective decay rate of the charge separated state. The experimental data in Figure 6 can obviously not be described by eq 4.

The observed (at least) biphasic decrease (Figure 6, inset) indicates that there are (at least) two fractions with rather different lifetimes of the charge separated state. Fraction B which disappears at low light intensities presumably represents PS I complexes with rather efficient electron transfer from A_1^- to F_X, forming predominantly the state $P700^+F_X^-$ with a rather long lifetime. Fraction *C* with a much shorter lifetime of the charge-separated state presumably represents PS I complexes where electron transfer from A_1^- to F_X is inefficient so that $P700^+A_1^-$ recombination ($t_{1/2} \cong 200$ μs) dominates. Much higher intensities are required to accumulate the charge-separated state in this fraction.

It should also be mentioned that the biphasic reoxidation kinetics of A_1^- at around 180 K (see Figure 1, 180 K trace) cannot be explained by a simple competition between forward electron transfer to F_X and recombination with $P700^+$ (such a situation should yield a monophasic decay of A_1^- with a rate corresponding to the sum of the two competing rate constants). Presumably the biphasic kinetics of A_1^- at around 180 K is a manifestation of the heterogeneity of electron transfer from A_1^- to F_X: the faster and slower phases would represent fractions B and C, respectively.

A Possible Origin of the Heterogeneity at Low Temperature. It has been proposed that PS I is frozen in different conformational substates and that the free energy of a given radical pair (e.g., $P700^+F_X^-$) varies between these substates (*2*, *20*). As the driving force for electron transfer from A_1^- to F_X is presumably rather small (for a discussion see ref 2), a variation of the free energy of the pair $P700^+F_X^-$ (and/or $P700^+A_1^-$) could give rise to a situation where electron transfer from A_1^- to F_X would be uphill (and hence virtually impossible at low temperatures) in some fraction of the PS I complexes, and downhill in another fraction. For electron transfer from F_X^- to F_A or F_B, the driving force, $-\Delta G°$, is on the order of 150 meV, as estimated from the reduction midpoint potentials at room temperature. This value could decrease considerably upon freezing because the stabilization of F_A^- and F_B^- by reorganization of the medium (e.g., diffusion and reorientation of water dipoles in the aqueous phase surrounding the acceptor side of PS I) should be strongly reduced when the suspension medium becomes solid. This effect of freezing combined with a variation of the driving force for electron transfer from F_X^- to F_A or F_B between different frozen conformational substates may yield a fraction of PS I complexes where this electron-transfer step would be uphill at low temperature.

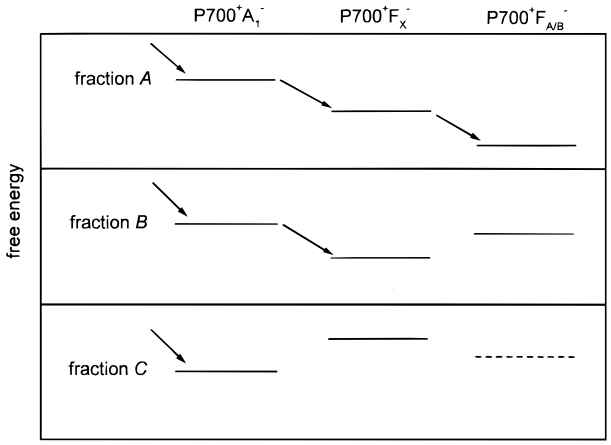

FIGURE 10: Free energy level scheme of the intermediate states $P700^+A_1^-$, $P700^+F_X^-$, and $P700^+F_{A/B}^-$ drawn for the three fractions A, B, and C of PS I complexes attributed to different conformational substates of PS I at low temperature. The data do not yield information on the free energy of $P700^+F_{A/B}^-$ in fraction C. This level is, therefore, depicted by a dashed line. Possible electron-transfer processes in the three fractions are indicated by arrows. For details see text.

Figure 10 illustrates the three energetic situations which may correspond to the three fractions A, B, and C introduced above. Each of these fractions may be composed of further substates, and this may lead to a wide distribution of electron transfer rates. Of course, in addition to the energy levels, other parameters which influence electron-transfer rates (the reorganization energy and in particular the distances between the redox cofactors) may vary between different frozen substates of the PS I complex, and this may contribute to the distribution of the electron-transfer rates as well. However, we favor a variation of the free-energy gap for electron transfer as the major origin of the heterogeneous photochemistry of PS I at low temperature, because the variation in the distances would have to be rather large to account for the observation that the forward electron transfer is virtually blocked in a fraction of PS I (according to Moser and Duttton (*35*), the rate of intraprotein electron transfer decreases by 1 order of magnitude every 1.7 Å).

The Transition from Efficient Forward Electron Transfer to Secondary Pair Recombination and Heterogeneity. The data presented in Figure 7, Figure 8, and Table 1 suggest that the transition from efficient forward electron transfer to secondary pair recombination is correlated with the liquid to glass transition of the suspension medium. When the liquid to glass transition is approached from higher temperatures, the viscosity of the medium increases dramatically. The temperature at which the viscosity reaches 10^{13} poise is called the glass transition temperature, T_g. Relaxation

processes slow in parallel (*40*). For example, for pure glycerol ($T_g \approx 185$ K) a large part of the dielectric relaxation occurs on a time scale of about 1 ns at 300 K, 10 μs at 230 K, 100 ms at 200 K, and 10^3 s at 184 K (*41*, *42*) (note that dielectric relaxation is a multiphasic process, i.e., some relaxation occurs on faster time scales).

The internal dynamics of proteins can be influenced by the viscosity of the medium in which the protein is suspended. Interestingly, some of the relaxation processes in myoglobin are arrested near the glass transition of the solvent (*30*, *43*). This has been called a slaved glass transition of the protein (*30*). The freezing of protein motions can affect electron transfer through changes in the free-energy gap and the reorganization energy (*44*). At temperatures below the glass transition, frozen-in conformational substates characterized by a wide distribution of rate constants due to different driving forces and/or reorganization energies will give rise to a heterogeneity of the electron-transfer processes at low temperature.

In more detail, we would like to propose two (nonalternative) mechanisms by which these changes of the physical properties of the suspension medium might affect electron transfer within the PS I complex.

1. Part of the energetic stabilization of the reduced states of the outermost electron acceptors due to dielectric relaxation of the suspension medium in response to the charge separation (see previous section) could be lost upon glass transition. Combined with some energetic variation of the energy levels of the charge-separated states due to different conformational substates, this could explain the heterogeneity giving rise to the fractions A, B, and C described above (see also Figure 10).

2. Provided that electron transfer to the terminal acceptors is accompanied at physiological conditions by large conformational changes of the subunit(s) exposed to the stroma, glass formation of the suspension medium could block these changes with the same consequences as described for mechanism 1.

Whatever the mechanism by which glass formation of the suspension medium affects forward electron transfer in PS I, our results give direct evidence that reorganization processes in the medium surrounding PS I play an important role for an efficient electron transfer beyond A_1 under normal in vivo conditions. The same reorganization processes may be responsible for the relatively high reorganization energy of electron transfer from A_1^- to F_X ($\lambda \cong 1$ eV, see above).

In contrast to forward electron transfer, charge recombination between $P700^+$ and A_1^- was only marginally affected by temperature, even at around the glass transition temperatures of the different glass-forming solvents (Figure 9). The general temperature independence (the rate increased only slightly upon cooling from about 3×10^3 s^{-1} at room temperature to about 4×10^3 s^{-1} at 5 K) can be explained if the energy $\hbar\omega$ of the nuclear vibration coupled to this electron transfer largely exceeds k_BT, as suggested for electron-transfer reactions in bacterial reaction centers (*33*). The absence of major effects at around the glass transitions on the $P700^+$ A_1^- recombination rate may be ascribed to various reasons. (i) Variations of the driving force between different conformational substates (i.e., the width of the distribution) are probably small compared to the large free-energy gap of the charge recombination between $P700^+$ and A_1^- (≈ -1.2 eV). (ii) P700 and A_1 are located more in the protein interior compared to the iron−sulfur clusters. Interior protein reorganization following electron transfer is presumably less affected by the freezing of the suspension medium. In addition, the larger distance should attenuate the contribution of dielectric relaxation of the suspension medium to the total reorganization energy.

ACKNOWLEDGMENT

We thank Dr. P. Fromme for providing the PS I complexes which were skillfully prepared by Ms. D. DiFiore and Ms. C. Otto.

REFERENCES

1. Golbeck, J. H. (1994) in *The Molecular Biology of Cyanobacteria* (Bryant, D. A., Ed.) pp 319−360, Kluwer Academic Publishers, Dordrecht.
2. Brettel, K. (1997) *Biochim. Biophys. Acta 1318*, 322−373.
3. Boekema, E. J., Dekker, J. P., van Heel, M. G., Rögner, M., Saenger, W., Witt, I., and Witt, H. T. (1987) *FEBS Lett. 217*, 283−286.
4. Kruip, J., Bald, D., Boekema, E., and Rögner, M. (1994) *Photosynth. Res. 40*, 279−286.
5. Krauss, N., Schubert, W.-D., Klukas, O., Fromme, P., Witt, H. T., and Saenger, W. (1996) *Nat. Struct. Biol. 3*, 965−973.
6. Schubert, W.-D., Klukas, O., Krauss, N., Saenger, W., Fromme, P., and Witt, H. T. (1997) *J. Mol. Biol. 272*, 741−769.
7. Zech, S. G., Lubitz, W., and Bittl, R. (1996) *Ber. Bunsen-Ges. Phys. Chem. 100*, 2041−2044.
8. Dzuba, S. A., Hara, H., Kawamori, A., Iwaki, M., Itoh, S., and Tsvetkov, Y. D. (1997) *Chem. Phys. Lett. 264*, 238−244.
9. Bittl, R., and Zech, S. G. (1997) *J. Phys. Chem. B 101*, 1429−1436.
10. Bittl, R., Zech, S. G., Fromme, P., Witt, H. T., and Lubitz, W. (1997) *Biochemistry 36*, 12001−12004.
11. MacMillan, F., Hanley, J., van der Weerd, L., Knupling, M., Un, S., and Rutherford, A. W. (1997) *Biochemistry 36*, 9297−9303.
12. van der Est, A., Prisner, T., Bittl, R., Fromme, P., Lubitz, W., Möbius, K., and Stehlik, D. (1997) *J. Phys. Chem. B 101*, 1437−1443.
13. Brettel, K. (1988) *FEBS Lett. 239*, 93−98.
14. Mathis, P., and Sétif, P. (1988) *FEBS Lett. 237*, 65−68.
15. Sétif, P., and Brettel, K. (1993) *Biochemistry 32*, 7846−7854.
16. Lüneberg, J., Fromme, P., Jekow, P., and Schlodder, E. (1994) *FEBS Lett. 338*, 197−202.
17. van der Est, A., Bock, C., Golbeck, J., Brettel, K., Sétif, P., and Stehlik, D. (1994) *Biochemistry 33*, 11789−11797.
18. Moënne-Loccoz, P., Heathcote, P., Maclachlan, D. J., Berry, M. C., Davis, I. H., and Evans, M. C. W. (1994) *Biochemistry 33*, 10037−10042.
19. Sétif, P., Mathis, P., and Vänngård, T. (1984) *Biochim. Biophys. Acta 767*, 404−414.
20. Schlodder, E., Brettel, K., Falkenberg, K., and Gergeleit, M. (1995) in *Photosynthesis: from light to Biospere* (Mathis, P., Ed.) Vol. 2, pp 107−110, Kluwer Academic Publishers, Dordrecht.
21. Witt, I., Witt, H. T., Gerken, S., Saenger, W., Dekker, J. P., and Rögner, M. (1987) *FEBS Lett. 221*, 260−264.
22. Brettel, K. (1989) *Biochim. Biophys. Acta 976*, 246−249.
23. Gerken, S., Brettel, K., Schlodder, E., and Witt, H. T. (1987) *FEBS Lett. 219*, 207−211.
24. Schlodder, E., and Meyer, B. (1987) *Biochim. Biophys. Acta 890*, 23−31.
25. Brettel, K., Sétif, P., and Mathis, P. (1986) *FEBS Lett. 203*, 220−224.
26. Ke, B. (1972) *Arch. Biochem. Biophys. 152*, 70−77.
27. Malkin, R., and Bearden, A. J. (1971) *Proc. Natl. Acad. Sci. U.S.A. 68*, 16−19.

28. Rasmussen, D. H., and MacKenzie, A. P. (1971) *J. Chem. Phys. 75*, 967−973.
29. Rasmussen, D. H., and MacKenzie, A. P. (1968) *Nature 220*, 1315−1317.
30. Iben, I. E. T., Braunstein, D., Doster, W., Frauenfelder, H., Hong, M. K., Johnson, J. B., Luck, S., Ormos, P., Schulte, A., Steinbach, P. J., Xie, A. H., and Young, R. D. (1989) *Phys. Rev. Lett. 62*, 1916−1919.
31. Sétif, P., Mathis, P., Lagoutte, B., and Duranton, J. (1984) in *Advances in Photosynthesis Research* (Sybesma, C., Ed.) Vol. 1, pp 589−592, Martinus Nijhoff/Dr. Junk Publishers, The Hague.
32. Marcus, R. A., and Sutin, N. (1985) *Biochim. Biophys. Acta 811*, 265−322.
33. Moser, C. C., Keske, J. M., Warncke, K., Farid, R. S., and Dutton, P. L. (1992) *Nature 355*, 796−802.
34. DeVault, D. (1980) *Q. Rev. Biophys. 13*, 387−978.
35. Moser, C. C., and Dutton, P. L. (1992) *Biochim. Biophys. Acta 1101*, 171−176.
36. Stehlik, D., van der Est, A., and Kamlowski, A. (1996) *Ber. Bunsen-Ges. Phys. Chem. 100*, 2028−2035.
37. Kamlowski, A. (1997) Ph.D. Thesis, Technische Universität Berlin, Germany.
38. Adman, E. T., Sieker, L. C., and Jensen, L. H. (1976) *J. Biol. Chem. 251*, 3801−3806.
39. Krishtalik, L. I. (1989) *Biochim. Biophys. Acta 977*, 200−206.
40. Wong, J., and Angell, C. A. (1976) *Glass structure by spectroscopy*, Dekker, New York.
41. Menon, N., O'Brien, K. P., Dixon, P. K., Wu, L., Nagel, S. R., Williams, B. D., and Carini, J. P. (1992) *J. Non-Cryst. Solids 141*, 61−65.
42. Schulz, A. K. (1954) *Kolloid-Z. 138*, 75−80.
43. Ansari, A., Jones, C. M., Henry, E. R., Hofrichter, J., and Eaton, W. A. (1992) *Science 256*, 1796−1798.
44. Kakitani, T., and Mataga, N. (1989) *Photosynth. Res. 22*, 187−193.

BI973182R